Tin-Vacancy Quantum Emitters in Diamond

Takayuki Iwasaki,[1,*] Yoshiyuki Miyamoto,[2] Takashi Taniguchi,[3] Petr Siyushev,[4] Mathias H. Metsch,[4] Fedor Jelezko,[4,5] and Mutsuko Hatano[1]

[1]*Department of Electrical and Electronic Engineering, Tokyo Institute of Technology, Meguro, Tokyo 152-8552, Japan*

[2]*Research Center for Computational Design of Advanced Functional Materials, National Institute for Advanced Industrial Science and Technology, Tsukuba 305-8568, Japan*

[3]*Research Center for Functional Materials, National Institute for Materials Science, 1-1 Namiki, Tsukuba 305-0044, Japan*

[4]*Institute for Quantum Optics, Ulm University, Ulm D-89081, Germany*

[5]*Center for Integrated Quantum Science and Technology (IQ^{ST}), Ulm University, Ulm D-89081, Germany*

(Received 14 August 2017; published 22 December 2017)

Tin-vacancy (Sn-V) color centers were created in diamond via ion implantation and subsequent high-temperature annealing up to 2100 °C at 7.7 GPa. The first-principles calculation suggested that a large atom of tin can be incorporated into a diamond lattice with a split-vacancy configuration, in which a tin atom sits on an interstitial site with two neighboring vacancies. The Sn-V center showed a sharp zero phonon line at 619 nm at room temperature. This line split into four peaks at cryogenic temperatures, with a larger ground state splitting (∼850 GHz) than that of color centers based on other group-IV elements, i.e., silicon-vacancy (Si-V) and germanium-vacancy (Ge-V) centers. The excited state lifetime was estimated, via Hanbury Brown–Twiss interferometry measurements on single Sn-V quantum emitters, to be ∼5 ns. The order of the experimentally obtained optical transition energies, compared with those of Si-V and Ge-V centers, was in good agreement with the theoretical calculations.

DOI: 10.1103/PhysRevLett.119.253601

The use of point defect-related color centers in solid-state materials is a promising approach for quantum information processing [1,2]. Nitrogen-vacancy (N-V) centers in diamond have been studied most intensively from the viewpoint of both fundamental and applied sciences [3,4]. However, the zero-phonon line (ZPL) of a N-V center constitutes a fraction of only 4% in its total fluorescence due to its large phonon sideband (PSB). Additionally, the N-V center is susceptible to external noise, leading to instability of the optical transition energy. To overcome these drawbacks, color centers based on group-IV elements, i.e., silicon-vacancy (Si-V) [5–7] and germanium-vacancy (Ge-V) [8–11] centers, have attracted attention because of their large ZPLs, structural symmetries that are resistant to external noise, and the availability of quantum emission from single centers. Recently, spin control and spin coherence time have been investigated for these two color centers [12–18], revealing that their spin coherence times are limited to submicroseconds even at cryogenic temperatures of 2–5 K, being much shorter than that of the N-V center [19,20]. This limitation originates from phonon-mediated transitions between the lower and upper branches in the ground state [13–16]. Further cooling down to the sub-Kelvin regime or strain engineering has been considered as a potential solution [15,16]. Very recently, both solutions have been attempted for Si-V [21–23]. Particularly, in Ref. [23] long spin coherence time in the order of milliseconds was achieved at sub-Kelvin temperatures in a dilution refrigerator. Another possible way to achieve a long spin coherence time even at a high temperature is the creation of a novel color center possessing a larger energy split in the ground state. For this purpose, in this study, we investigated the utilization of a group-IV atom of tin [Sn, Fig. 1(a)]. We fabricated tin-vacancy (Sn-V) centers in diamond in both ensemble and single states via a combination of ion implantation and subsequent high-temperature annealing up to 2100 °C under a high pressure of 7.7 GPa. Low-temperature optical measurements revealed that the ground state splitting of the Sn-V center was much larger than that of the Si-V and Ge-V centers. The atomic structure and optical transition energy were calculated via first-principles calculations, with comparison to Si-V and Ge-V centers.

Figure 1(b) shows a room temperature photoluminescence (PL) spectrum from ensemble Sn-V centers, annealed at 2100 °C at 7.7 GPa after Sn ion implantation, with a dose of 2×10^{13} cm^{-2}, into diamond (see Supplemental Material [24] for experimental details). The Sn-V centers exhibit a sharp and strong ZPL at 619 nm, with a full width at half maximum (FWHM) of 6.2 nm and with the accompanying PSB. We investigated the effect of the postimplantation annealing temperature on the activation of the Sn-V centers. Figure 1(c) shows the temperature dependence of the ZPL linewidth in the Sn-V spectrum. We performed the annealing under vacuum or high-pressure conditions for 30 min. The increase in the annealing temperature effectively reduced the FWHM irrespective of the annealing environments. Significantly, the high pressure of 7.7 GPa enabled us to reach a temperature of 2100 °C while avoiding graphitization of the

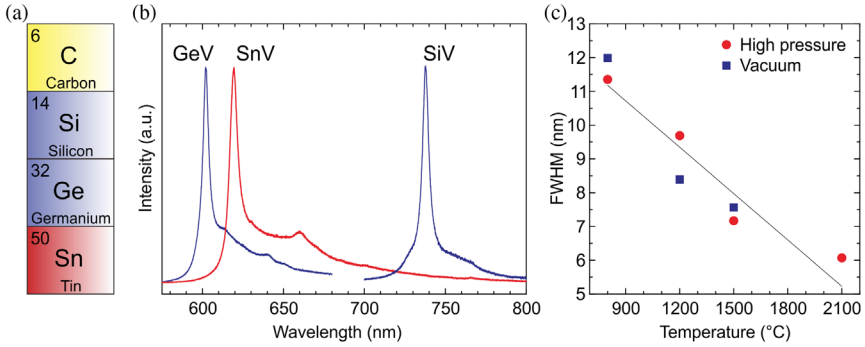

FIG. 1. Activation and optical properties of ensemble Sn-V centers. (a) The group-IV periodic table. (b) Room temperature PL spectrum from ensemble of Sn-V centers, annealed at 2100 °C after ion implantation with a dose of 2×10^{13} cm^{-2} at an acceleration energy of 130 keV. PL spectra from ensemble of Si-V and Ge-V centers are also shown. (c) Dependence of linewidth of ZPL from Sn-V on the postimplantation annealing temperature under a high vacuum of $\sim 10^{-5}$ Pa or high pressure of 7.7 GPa.

diamond [29,30]. Consequently, the linewidth was reduced from ~12 nm at 800 °C to ~6 nm at 2100 °C by suppressing inhomogeneous broadening due to surrounding defects and strain in the atomic structure induced during ion implantation. Furthermore, such a high-temperature treatment is important for suppressing the formation of undesirable fluorescent structures. Although two prominent peaks with unknown origins were observed at 595 and 646 nm at temperatures of 1500 °C and lower, they were annealed out by the treatment at 2100 °C (Supplemental Material [24]). The large Sn atom is thought to be less movable in the diamond lattice and to produce a number of vacancies during ion implantation. Thus, the high-temperature treatment is required to selectively activate the high-quality Sn-V centers.

Low-temperature PL measurements were performed to reveal the fine structure of the Sn-V center [Fig. 2(a)]. Only one peak was observed at room temperature; it split into two peaks with a FWHM of approximately 0.2 nm (155 GHz) at 4 K. This linewidth is broader than the lifetime-limited linewidth of 32 MHz. This was caused by the remaining implantation damages created via the high-dose process, not being fully recovered even via the high-temperature treatment under high pressure. The linewidth is expected to be further reduced by a longer annealing time and/or higher-temperature treatment. Additionally, in further studies, photoluminescence excitation spectroscopy on a low-dose sample will be useful to reveal the natural linewidth.

To investigate the fine structure in detail, the temperature dependence of the PL spectrum was recorded [Fig. 2(b)]. When increasing the temperature, another two peaks (denoted as A and B) appeared in a higher energy region in addition to the peaks seen at 4 K (denoted as C and D). The intensities of peaks A and B become larger as the temperature increases. This fact suggests that the Sn-V center has an energy level structure composed of four levels with split ground and excited states [Fig. 2(c)]. The ground and excited state splittings of the Sn-V center are ~850 and ~3000 GHz, respectively, being much larger than those of Si-V and Ge-V centers possessing the same four-level structure [5,9]. Note that the population of the upper branch excited from the lower branch exponentially decreases with the excited state splitting [5,9], as illustrated by the low PL intensities of peaks A and B even at a high temperature of 100 K (compared with Si-V [5] and Ge-V [9]).

In Fig. 2(d), we summarize the splittings as a function of the spin-orbit coupling constant [31] of the group-IV

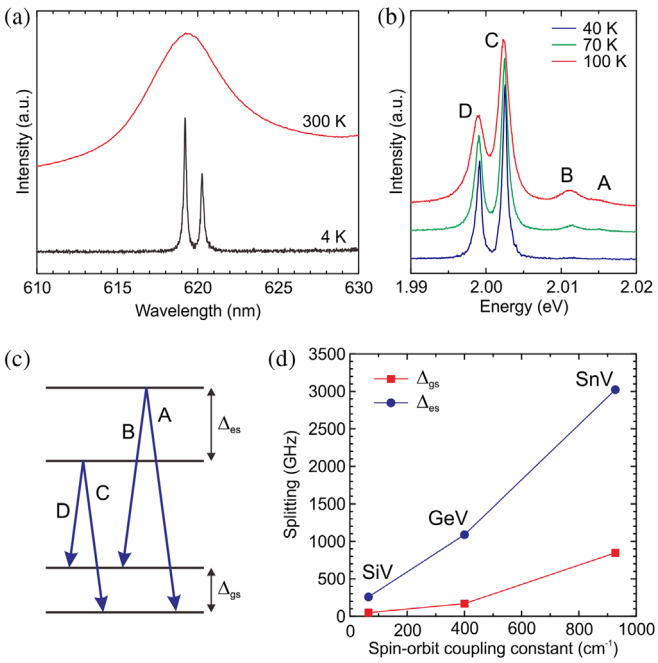

FIG. 2. Low-temperature optical characteristics. (a) ZPL of ensemble Sn-V centers at room temperature and at 4 K. The spectrometer resolution is approximately 0.04 nm. Thus, the observed linewidth of 0.2 nm at 4 K is not spectrometer limited. (b) PL spectra at different measurement temperatures. (c) Fine structure. (d) Ground and excited state splittings as a function of the spin-orbit coupling constant of the group-IV element. The values of the Si-V and Ge-V centers were adapted from Refs. [5] and [9], respectively.

elements. Both the ground and excited state splittings increase as the spin-orbit coupling constant of the elements increases. The ground state splitting of the Sn-V center is 17 and 5 times larger than that of Si-V and Ge-V, respectively. The observed splittings should be originated not only from the spin-orbit coupling constant of the group-IV elements, but also from the degree of the hybridization of the p orbitals of the elements with carbon dangling bonds (Indeed, a minor contribution of the valence p states of the group-IV impurity to the occupied orbital states was reported in Ref. [32], see also the Supplemental Material [24]). In addition, the dynamic Jahn-Teller effect would also contribute to the splittings, as observed in the Si-V centers [33]. Its contribution to the splittings will be revealed by observing the fine structures under magnetic fields [33].

We next fabricated single Sn-V color centers with a lower Sn ion dose of 2×10^8 cm^{-2}. The inset in Fig. 3(a) shows a confocal fluorescence microscopy image of an isolated Sn-V center with an FWHM of ~450 nm. The PL spectrum was recorded at the bright spot and background position in Fig. 3(a). The bright spot clearly shows a ZPL with a linewidth of 6 nm from the Sn-V center. The background position also shows multiple peaks in the same region, but they originate from the second-order Raman scattering from the diamond (611 and 620 nm) and probably a surface defect (630 nm), which is not visible in the bulk diamond region. The background-subtracted PL shows the ZPL and PSB from only the Sn-V center. We performed the Hanbury Brown–Twiss interferometry [34] measurements to confirm that the observed spots correspond to a single Sn-V center. Figure 3(b) shows the results of a second-order autocorrelation function, $g^2(\tau)$, for different excitation laser powers. Because of the background emission, $g^2(0)$ becomes ~0.5 [the right axis in Fig. 3(b)]. Thus, we corrected the background level using the relation $g^2_{\mathrm{corr}}(\tau) = [g^2(\tau) - (1-\rho^2)]/\rho^2$ [35], where $\rho = S/(S+B)$. S is the intensity of the Sn-V center, and B is the background intensity. ρ takes values of approximately 0.7. As shown along the left axis in Fig. 3(b), $g^2_{\mathrm{corr}}(0)$ almost reaches zero at a delay time of 0 ns, which is an unambiguous proof of single photon emission [36]. The data were fitted using the equation $g^2_{\mathrm{corr}}(\tau) = 1 - (1+\alpha)e^{-(|\tau|/\tau_1)} + \alpha e^{-(|\tau|/\tau_2)}$ [37], where α, τ_1, and τ_2 are fitting parameters. At low excitation powers, τ_1 yields an estimated excited state lifetime of a fluorescent structure. The two emitters investigated in this study show a τ_1 value of ~5 ns (another emitter is shown in the Supplemental Material [24]). For all the laser powers used here, $g^2(\tau)$ exhibits a bunching behavior observed as $g^2(\tau)$ over unity. This means that the Sn-V center possesses a shelving state in addition to the ground and excited states, or that photoionization occurs during the laser excitation [37].

The fluorescence intensity was measured as a function of the laser power [Fig. 3(c)]. We used two kinds of filters: the ZPL intensity alone, which was recorded using a band pass filter (BPF) with a 20 nm width around the ZPL, and the intensity from the whole Sn-V spectrum (ZPL + PSB), which was recorded using a 600 nm long pass filter. Both curves show nonlinear behavior at high laser powers. The plots were fitted using the equation $I = I_\infty P/(P + P_{\mathrm{sat}})$ [6], where I_∞ and P_{sat} are the saturation intensity and saturation power, respectively. The saturation intensities of the ZPL and whole spectrum are 280 and 530×10^3 counts/s, respectively. Note that we used an air objective (numerical aperture or NA of 0.95) here; thus, the utilization of a higher NA oil objective and/or microcavity structures [38–41] will enhance the efficiency of collecting light from the emitter and lead to a further increase in the saturation intensity. Importantly, the Sn-V center shows a higher fluorescence intensity than that of Si-V (56×10^3 counts/s observed using a 0.95-NA objective [42]) despite the longer excited state lifetime compared

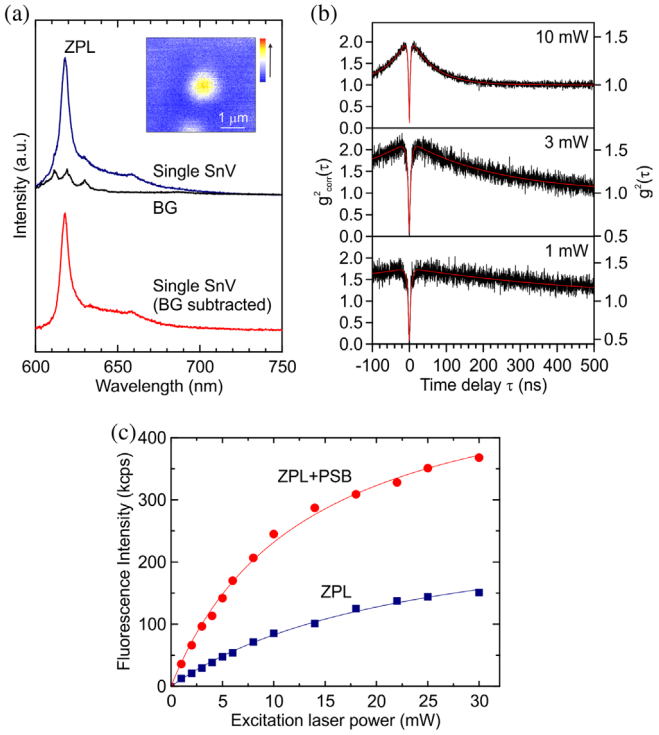

FIG. 3. Single Sn-V color center. (a) PL spectrum for the isolated Sn-V center shown in inset. Inset: confocal fluorescence microscopy image taken using a BPF with a width of 20 nm around the ZPL. BG denotes the PL at the background position, where no Sn-V center exists. The bottom curve is the background-subtracted single Sn-V spectrum. (b) Background corrected second-order autocorrelation function, $g^2_{\mathrm{corr}}(\tau)$, at different excitation laser powers, measured using a BPF. (c) Saturation curves of the ZPL only and of the whole spectrum. The background intensities were subtracted from each curve (see Supplemental Material [24]). The single Sn-V centers were fabricated via ion implantation (dose: 2×10^8 cm^{-2}, acceleration energy: 150 keV) and annealing at 2100 °C under a high pressure of 7.7 GPa. All measurements were made with an air objective (NA of 0.95) at room temperature.

with Si-V ($1 \sim 2$ ns [6,42]). This implies a high quantum efficiency of the Sn-V center. We estimated the quantum efficiency based on the rate equations modeled in Ref. [43] and obtained ~0.8 (see Supplemental Material [24]). This value is comparable to that of the N-V center (0.7-1 [43,44]) and higher than that of the Si-V center (~0.3 in bulk diamond [45] and <0.1 in nanodiamonds [46]). It is worth noting that the comparison of the fluorescence intensities of the ensemble with the single Sn-V center provides a conversion efficiency from Sn ions to Sn-V centers of approximately 1%–2%. Counting bright spots in confocal microscope images of the single Sn-V sample, observed with a 620 nm BPF, gives rise to ~4%, which is roughly the same level as that of the estimation made using the ensemble.

We performed first-principles calculations of the atomic structure, energy levels, and optical transition energy of the Sn-V center (see Supplemental Material [24] for calculation details). Figure 4(a) shows the optimized atomic configuration of a Sn-V center with a split-vacancy structure. When we start the calculation from a structure with a Sn atom at a substitutional position with a neighboring vacancy (with the same C_{3v} symmetry as that of the N-V center), the Sn atom is relaxed to an interstitial site upon structural optimization. Consequently, the Sn atom sits at an interstitial site between two vacancies at carbon lattice sites. This structure possesses the same D_{3d} symmetry as that of the Si-V and Ge-V centers. In accordance with the order of atomic sizes, the nearest C-Si, C-Ge, and C-Sn distances are

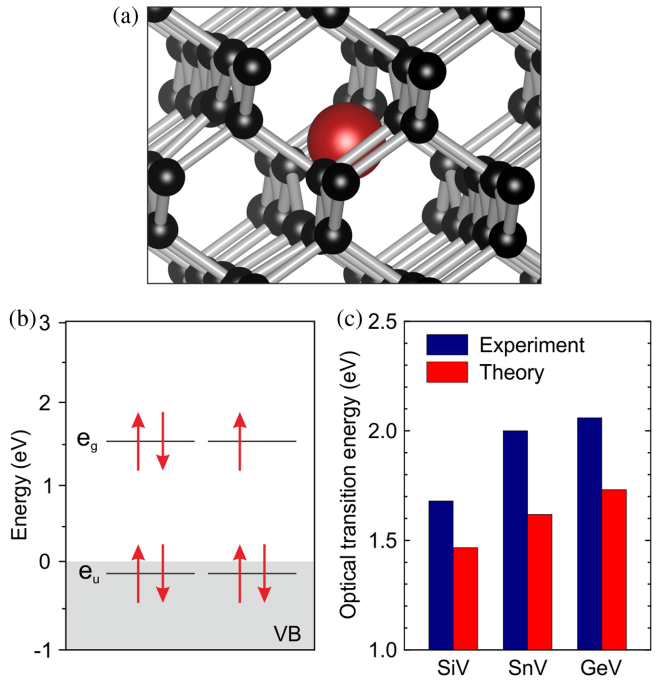

FIG. 4. Theoretical calculation of the Sn-V center via first-principles calculation. (a) Atomic structural model. The red sphere and black spheres denote the Sn atom and C atoms, respectively. (b) Energy levels of the ground state. VB denotes the valence band of diamond. (c) Optical transition energies.

1.94, 2.05, and 2.14 Å, respectively. The energy levels of the ground state of the Sn-V center, assuming a negatively charged state, are shown in Fig. 4(b). The transition energy between the negatively charged and neutral states is located below the midgap in the energy gap of the diamond [47], implying that the Sn-V takes the negatively charged state in the high-purity IIa-type diamond crystals used in this study. The degenerated e_u levels are fully occupied, while one of the degenerated e_g levels is half-occupied. Upon optical excitation, one electron with a down spin in the e_u level is pumped up to the e_g level and then relaxes back while emitting photons with an energy of ~2 eV.

Here, we discuss the optical transition energy of the color centers based on the group-IV elements. Interestingly, the order of the optical transition energy is not proportional to the atomic size of the element. As shown in Fig. 1(b), the Si-V centers exhibit a ZPL at 738 nm, while the Ge-V centers composed of a larger atom exhibit a higher transition energy at 602 nm. However, the ZPL energy of the Sn-V centers with an even heavier atom is less than that of the Ge-V center. The transition energy of Sn-V was calculated using the structural model shown in Fig. 4(a) and is shown, along with the transition energies for Si-V and Ge-V, in Fig. 4(c), which also includes the experimental ZPL transition energies. The experimental order of the optical excitation gap (Si-V < Sn-V < Ge-V) is consistent with the theoretical results, which was also reported by Goss *et al.* [47].

Finally, we discuss the expected spin coherence time of the Sn-V center. The phonon-mediated transition rate is proportional to the occupation of the phonon mode, $n(\Delta_{\mathrm{g.s.}}, T) = 1/(e^{(h\Delta_{\mathrm{g.s.}}/k_B T)} - 1)$, where h and k_B are the Planck and Boltzmann constants, respectively [21,48]. The occupation decreases exponentially with $\Delta_{\mathrm{g.s.}}$ and temperature, leading to the significant reduction in the transition rate in the Sn-V center with the large ground state splitting of ~850 GHz compared with the Si-V and Ge-V centers (Supplemental Material [24]). Therefore, a long spin coherence time (in the range of milliseconds) can be expected for Sn-V without cooling down to the sub-Kelvin regime, which is necessary for Si-V [23].

We introduced large Sn atoms in the diamond lattice and obtained Sn-V centers with large level splitting in the ground state. The incorporation of a heavy atom in diamond will become more important from the viewpoints of materials science [49] and quantum optics. The fabrication of optical centers based on large atoms such as Eu [50], Xe [51], and Tl [52] has thus far been demonstrated. For further development of the heavy atom-related color centers, it is essential to achieve high-quality quantum emitters via an adequate process for each atom, such as high-temperature annealing under high pressure, as demonstrated in this study.

In conclusion, we have demonstrated the fabrication of both ensemble and single Sn-V centers in diamond via ion

implantation and annealing. The high annealing temperature of 2100 °C under a high pressure of 7.7 GPa led to narrow ZPLs from the Sn-V centers while annealing out undesirable fluorescent structures. Low-temperature optical measurements revealed that the Sn-V center possesses a four-level structure with large splitting in the ground state, i.e., ~850 GHz. In comparison to the Si-V and Ge-V centers, we showed that the magnitude of the splitting increases as the spin-orbit coupling (atomic number) of the group-IV element becomes larger. Our theoretical calculations indicated that the split-vacancy configuration of the Sn-V center is in agreement with the observed fine structures. The development of a color center with large ground state splitting is expected to provide a way to establish a quantum light-matter interface with a long spin coherence time.

This work was supported by JST-PRESTO (Grant No. JPMJPR16P2) and JST-CREST. We thank Shinji Nagamachi for supporting in ion implantation.

Note added.—Recently, we became aware of another study presenting the room temperature characteristics of Sn-related color centers in diamond [53].

iwasaki.t.aj@m.titech.ac.jp

[1] R. Hanson and D. Awschalom, Nature (London) **453**, 1043 (2008).
[2] I. Aharonovich, D. Englund, and M. Toth, Nat. Photonics **10**, 631 (2016).
[3] F. Jelezko and J. Wrachtrup, Phys. Status Solidi A **203**, 3207 (2006).
[4] T. Schröder, S. L. Mouradian, J. Zheng, M. E. Trusheim, M. Walsh, E. H. Chen, L. Li, I. Bayn, and D. Englund, J. Opt. Soc. Am. B **33**, B65 (2016).
[5] C. D. Clark, H. Kanda, I. Kiflawi, and G. Sittas, Phys. Rev. B **51**, 16681 (1995).
[6] C. Wang, C. Kurtsiefar, H. Weinfurter, and B. Burchard, J. Phys. B **39**, 37 (2006).
[7] A. Sipahigil, R. E. Evans, D. D. Sukachev, M. J. Burek, J. Borregaard, M. K. Bhaskar, C. T. Nguyen, J. L. Pacheco, H. A. Atikian, C. Meuwly, R. M. Camacho, F. Jelezko, E. Bielejec, H. Park, M. Lončar, and M. D. Lukin, Science **354**, 847 (2016).
[8] T. Iwasaki, F. Ishibashi, Y. Miyamoto, Y. Doi, S. Kobayashi, T. Miyazaki, K. Tahara, K. D. Jahnke, L. J. Rogers, B. Naydenov, F. Jelezko, S. Yamasaki, S. Nagamachi, T. Inubushi, N. Mizuochi, and M. Hatano, Sci. Rep. **5**, 12882 (2015).
[9] Y. N. Palyanov, I. N. Kupriyanov, Y. M. Borzdov, and N. V. Surovtsev, Sci. Rep. **5**, 14789 (2015).
[10] E. A. Ekimov, S. G. Lyapin, K. N. Boldyrev, M. V. Kondrin, R. Khmelnitskiy, V. A. Gavva, T. V. Kotereva, and M. N. Popova, JETP Lett. **102**, 701 (2015).
[11] M. K. Bhaskar, D. D. Sukachev, A. Sipahigil, R. E. Evans, M. J. Burek, C. T. Nguyen, L. J. Rogers, P. Siyushev, M. H. Metsch, H. Park, F. Jelezko, M. Lončar, and M. D. Lukin, Phys. Rev. Lett. **118**, 223603 (2017).
[12] T. Müller, C. Hepp, B. Pingault, E. Neu, S. Gsell, M. Schreck, H. Sternschulte, D. Steinmüller-Nethl, C. Becher, and M. Atatüre, Nat. Commun. **5**, 3328 (2014).
[13] B. Pingault, J. N. Becker, C. H. H. Schulte, C. Arend, C. Hepp, T. Godde, A. I. Tartakovskii, M. Markham, C. Becher, and M. Atatüre, Phys. Rev. Lett. **113**, 263601 (2014).
[14] L. J. Rogers, K. D. Jahnke, M. H. Metsch, A. Sipahigil, J. M. Binder, T. Teraji, H. Sumiya, J. Isoya, M. D. Lukin, P. Hemmer, and F. Jelezko, Phys. Rev. Lett. **113**, 263602 (2014).
[15] B. Pingault, D.-D. Jarausch, C. Hepp, L. Klintberg, J. N. Becker, M. Markham, C. Becher, and M. Atatüre, Nat. Commun. **8**, 15579 (2017).
[16] P. Siyushev, M. H. Metsch, A. Ijaz, J. M. Binder, M. K. Bhaskar, D. D. Sukachev, A. Sipahigil, R. E. Evans, C. T. Nguyen, M. D. Lukin, P. R. Hemmer, Y. N. Palyanov, I. N. Kupriyanov, Y. M. Borzdov, L. J. Rogers, and F. Jelezko, Phys. Rev. B **96**, 081201 (2017).
[17] J. N. Becker, J. Goerlitz, C. Arend, M. Markham, and C. Becher, Nat. Commun. **7**, 13512 (2016).
[18] Y. Zhou, A. Rasmita, K. Li, Q. Xiong, I. Aharonovich, and W. Gao, Nat. Commun. **8**, 14451 (2017).
[19] G. Balasubramanian, P. Neumann, D. Twitchen, M. Markham, R. Kolesov, N. Mizuochi, J. Isoya, J. Achard, J. Beck, J. Tissler, V. Jacques, P. R. Hemmer, F. Jelezko, and J. Wrachtrup, Nat. Mater. **8**, 383 (2009).
[20] N. Bar-Gill, L. M. Pham, A. Jarmola, D. Budker, and R. L. Walsworth, Nat. Commun. **4**, 1743 (2013).
[21] Y. Sohn, S. Meesala, B. Pingault, H. A. Atikian, J. Holzgrafe, M. Guendogan, C. Stavrakas, M. J. Stankey, A. Sipahigl, J. Choi, M. Zhang, J. L. Pacheco, J. Abraham, D. Bielejec, M. D. Lukin, M. Atatuere, and M. Loncar, arXiv:1706.03881.
[22] J. N. Becker, B. Pingault, D. Gross, M. Guendogan, N. Kukharchyk, M. Markham, A. Edmonds, M. Atatuere, P. Bushev, and C. Becher, arXiv:1708.08263.
[23] D. D. Sukachev, A. Sipahigil, C. T. Nguyen, M. K. Bhaskar, R. E. Evans, F. Jelezko, and M. D. Lukin, Phys. Rev. Lett. **119**, 223602 (2017).
[24] See Supplemental Material at http://link.aps.org/supplemental/10.1103/PhysRevLett.119.253601 for more information on conditions of experiments and theoretical calculations, effect of the annealing temperature, level splittings, saturation curves, quantum efficiency, and estimation of spin coherence time, which includes Refs. [25–28].
[25] M. Akaishi, H. Kanda, and S. Yamaoka, Jpn. J. Appl. Phys. **29**, L1172 (1990).
[26] N. Troullier and J. L. Martins, Phys. Rev. B **43**, 1993 (1991).
[27] J. P. Perdew, K. Burke, and M. Ernzerhof, Phys. Rev. Lett. **77**, 3865 (1996).
[28] Y. Nishida, Y. Mita, K. Mori, S. Okuda, S. Sato, S. Yazu, M. Nakagwa, and M. Okada, Mater. Sci. Forum **38-41**, 561 (1989).
[29] A. T. Collins, A. Connor, C.-H. Ly, and A. Shareef, J. Appl. Phys. **97**, 083517 (2005).
[30] B. Harte, T. Taniguchi, and S. Chakraborty, Mineral Mag. **73**, 201 (2009).
[31] S. Frage, J. Karwowski, and K. M. S. Saxene, *Handbook of Atomic Data* (Elsevier, New York, 1976).
[32] A. Gali and J. R. Maze, Phys. Rev. B **88**, 235205 (2013).

[33] C. Hepp, T. Müller, V. Waselowski, J. N. Becker, B. Pingault, H. Sternschulte, D. Steinmüller-Nethl, A. Gali, J. R. Maze, M. Atatüre, and C. Becher, Phys. Rev. Lett. **112**, 036405 (2014).
[34] R. Hanbury and R. Q. Twiss, Nature (London) **178**, 1046 (1956).
[35] R. Brouri, A. Beveratos, J.-P. Poizat, and P. Grangier, Opt. Lett. **25**, 1294 (2000).
[36] M. Leifgen, T. Schröder, F. Gädeke, R. Riemann, V. Métillon, E. Neu, C. Hepp, C. Arend, C. Becher, K. Lauritsen, and O. Benson, New J. Phys. **16**, 023021 (2014).
[37] S. Prawer and I. Aharonovich, *Quantum Information Processing with Diamond: Principles and Applications* (Woodhead Publishing, Cambridge, UK, 2014), Chap. 6.
[38] J. P. Hadden, J. P. Harrison, A. C. Stanley-Clarke, L. Marseglia, Y.-L. D. Ho, B. R. Patton, J. L. O'Brien, and J. G. Rarity, Appl. Phys. Lett. **97**, 241901 (2010).
[39] M. Jamali, I. Gerhardt, M. Rezai, K. Frenner, H. Fedder, and J. Wrachtrup, Rev. Sci. Instrum. **85**, 123703 (2014).
[40] T. M. Babinec, B. J. M. Hausmann, M. Khan, Y. Zhang, J. R. Maze, P. R. Hemmer, and M. Lončar, Nat. Nanotechnol. **5**, 195 (2010).
[41] S. Furuyama, K. Tahara, T. Iwasaki, M. Shimizu, J. Yaita, M. Kondo, T. Kodera, and M. Hatano, Appl. Phys. Lett. **107**, 163102 (2015).
[42] L. J. Rogers, K. D. Jahnke, T. Teraji, L. Marseglia, C. Mueller, B. Naydenov, H. Shauffert, C. Kranz, J. Isoya, L. P. McGuinness, and F. Jelezko, Nat. Commun. **5**, 4739 (2014).
[43] M. Berthel, O. Mollet, G. Dantelle, T. Gacoin, S. Huant, and A. Drezet, Phys. Rev. B **91**, 035308 (2015).
[44] J. Wrachtrup and F. Jelezko, J. Phys. Condens. Matter **18**, S807 (2006).
[45] J. N. Becker and C. Becher, Phys. Status Solidi A **214**, 1700586 (2017).
[46] E. Neu, M. Agio, and C. Becher, Opt. Express **20**, 19956 (2012).
[47] J. P. Goss, P. R. Briddon, M. J. Rayson, S. J. Sque, and R. Jones, Phys. Rev. B **72**, 035214 (2005).
[48] K. D. Jahnke, A. Sipahigil, J. M. Binder, M. W. Doherty, M. Metsch, L. J. Rogers, N. B. Manson, M. D. Lukin, and F. Jelezko, New J. Phys. **17**, 043011 (2015).
[49] V. Nadolinny, A. Komarovskikh, and Y. Palyanov, Crystals **7**, 237 (2017).
[50] A. Magyar, W. Hu, T. Shanley, M. E. Flatte, E. Hu, and I. Aharonovich, Nat. Commun. **5**, 3523 (2014).
[51] R. Sandstrom, L. Ke, A. Martin, Z. Wang, M. Kianinia, B. Green, W.-B. Gao, and I. Aharonovich, arXiv: 1704.01636.
[52] A. M. Zaitsev, Phys. Rev. B **61**, 12909 (2000).
[53] S. D. Tchernij, T. Herzig, J. Forneris, J. Küpper, S. Pezzagna, P. Traina, E. Moreva, I. P. Degiovanni, G. Brida, N. Skukan, M. Genovese, M. Jakšić, J. Meijer, and P. Olivero, ACS Photonics **4**, 2580 (2017).